J Mater Sci: Mater Med (2008) 19:1693–1702
DOI 10.1007/s10856-007-3252-x

# The thermal stability of hydroxyapatite in biphasic calcium phosphate ceramics

**R. W. N. Nilen · P. W. Richter**

Received: 16 November 2006 / Accepted: 2 August 2007 / Published online: 25 September 2007


**Abstract** Biphasic calcium phosphate ceramics (BCP) comprising a mix of non-resorbable hydroxyapatite (HA) and resorbable $\beta$-tricalcium phosphate ($\beta$-TCP) are particularly suitable materials for synthetic bone substitute applications. In this study, HA synthesised by solid state reaction was mechanically mixed with $\beta$-TCP, then sintered to form a suite of BCP materials with a wide range of HA/$\beta$-TCP phase content ratios. The influence of sintering temperature and composition on the HA thermal stability was quantified by X-ray diffraction (XRD). The pre-sinter $\beta$-TCP content was found to strongly affect the post-sinter HA/$\beta$-TCP ratio by promoting the thermal decomposition of HA to $\beta$-TCP, even at sintering temperatures as low as 850 °C. For BCP material with pre-sinter HA/$\beta$-TCP = 40/60 wt%, approximately 80% of the HA decomposed to $\beta$-TCP during sintering at 1000 °C. Furthermore, the HA content appeared to influence the reverse transformation of $\alpha$-TCP to $\beta$-TCP expected upon gradual cooling from sintering temperatures greater than 1125 °C. Because the HA/$\beta$-TCP ratio dominantly determines the rate and extent of BCP resorption in vivo, the possible thermal decomposition of HA during BCP synthesis must be considered, particularly if high temperature treatments are involved.

R. W. N. Nilen · P. W. Richter (✉)
Materials Science and Manufacturing Unit,
Council for Scientific and Industrial Research,
P.O. Box 395, Pretoria 0001, South Africa
e-mail: wrichter@csir.co.za

## 1 Introduction

Biphasic calcium phosphate ceramics (BCP) generally comprise an intimate mix of non-resorbable hydroxyapatite (HA: $Ca_{10}(PO_4)_6(OH)_2$) and resorbable $\beta$-tricalcium phosphate ($\beta$-TCP: $\beta$-$Ca_3(PO_4)_2$) [1]. They are particularly suitable materials for synthetic bone substitute applications because the HA provides a permanent scaffold for new bone formation via osteoconduction (and in some special cases, osteoinduction [2]), and the resorption of the $\beta$-TCP oversaturates the local environment with $Ca^{2+}$ and $PO_4^{3-}$ ions to accelerate this new bone formation (see, e.g. [3] for a recent review). Many in vitro and in vivo studies have been carried out on BCP [1, 4–12], and a wide range of BCP products are now commercially available, e.g. MBCP® and Triosite® and Camceram®.

The HA/$\beta$-TCP phase content ratio dominantly determines the rate and extent of BCP resorption in vivo, in that higher $\beta$-TCP contents allow faster and more extensive resorption [1, 4, 13]. Ideally the resorption rate should match the rate of new bone formation, so the HA/$\beta$-TCP phase content ratio is a critical parameter to control during synthesis. Most BCP products have a $\beta$-TCP content of 40 wt% (balance HA), although Livingstone-Arinzeh et al. [6] recently reported that BCP with 80 wt% $\beta$-TCP content gave the highest rate of human mesenchymal stem cell-induced osteoinduction in an ectopic mouse model.

BCP is usually synthesised by either (i) mechanical mixing of HA and $\beta$-TCP powder, or (ii) sintering Ca-deficient apatite (general formula usually expressed as: $Ca_{10-x}(PO_4)_{6-x}(HPO_4)_x(OH)_{2-x}$, where $0 \le x \le 2$ [14]) that is formed by wet precipitation methods [5, 15–19]. Most studies have focussed on (ii), mainly because biphasic mixing on a crystallite level is possible with this method.

However, the Ca/P molar ratio of the precipitated powder (and subsequently the sintered material) depends very critically on the precipitation reaction pH and temperature, which can be difficult to control [20].

A crucial consideration when sintering BCP is the thermal stability of the phases. Much has been reported on the thermal stability of HA, particularly significant in high temperature sintering and plasma spraying applications [21–24]. An important reaction that has been reported at temperatures above 800 °C is the decomposition of HA to $\beta$-TCP (e.g. [21]):

$$Ca_{10}(PO_4)_6(OH)_2 \rightarrow 3\beta\text{-}Ca_3(PO_4)_2 + CaO + H_2O \quad (R1)$$

It is now generally accepted ([24, 25] and references contained therein) that this thermal decomposition of HA proceeds via the interim formation of firstly oxyhydroxyapatite, then oxyapatite (respectively, OHAP: $Ca_{10}(PO_4)_6(OH)_{2-2x}O_xV_x$ and OHA: $Ca_{10}(PO_4)_6O_xV_x$ where V stands for a lattice vacancy in the OH position along the crystallographic c-axis). OHA then finally converts to various TCP and CaO phases.

Also important is the decomposition of Ca-deficient apatite to $\beta$-TCP between 700 °C and 800 °C with the loss of water, according to the global reaction [17, 26]:

$$Ca_{10-x}(HPO_4)_x(PO_4)_{6-x}(OH)_{2-x} \rightarrow (1-x)Ca_{10}(PO_4)_6(OH)_2 + 3x\beta\text{-}Ca_3(PO_4)_2 + xH_2O \quad (R2)$$

As these thermal decomposition reactions bring about a change in the HA/$\beta$-TCP phase content ratio of the material, they will result in a change in its resorption rate in vivo. In addition, the presence of CaO and its subsequent transformation to $Ca(OH)_2$ can lead to internal stresses and cracking in the material due to the associated volume change [13]. Thus such reactions need to be avoided, or at least managed during BCP synthesis.

It is also well established that $\beta$-TCP transforms to $\alpha$-TCP above 1125 °C (see, e.g. [27] and references therein):

$$\beta\text{-}Ca_3(PO_4)_2 \rightarrow \alpha\text{-}Ca_3(PO_4)_2 \quad (R3)$$

The reverse transformation, $\alpha$-TCP → $\beta$-TCP, occurs upon gradual cooling, although this can be avoided, or at least reduced, by rapid thermal quenching.

The thermal stability of HA in BCP produced by mechanical mixing and sintering, however, has received relatively little attention, and hence is the focus of this study. The HA was synthesised by solid state reaction (a seldom published route), and the BCP was produced with a wide compositional range (0–100 wt% $\beta$-TCP, balance HA), then sintered at temperatures ranging from 850 °C to 1300 °C. X-ray diffraction (XRD), Fourier transform infrared spectroscopy (FTIR) and thermo-gravimetric analysis/simultaneous differential thermal analysis (TGA/SDTA) were used to characterise the pre-sinter and post-sinter material. Particular emphasis was placed on the quantification of the HA/$\beta$-TCP phase content ratios by XRD.

## 2 Materials and methods

### 2.1 HA powder preparation

HA was synthesised by solid state reaction [28, 29] between $\beta$-TCP (Merck No. 2143) and $Ca(OH)_2$ (Saarchem Univar No. 1525220). The starting powders were combined in appropriate quantities for a Ca/P molar ratio of 1.67 (the ratio for stochiometric HA), then mixed in deionised water using a high speed Silverson homogeniser for 20 min. The resulting slurry was gelled to prevent powder separation during drying at 100 °C for 15 h. The dried slurry was then reacted at 1000 °C for 18 h to produce HA by:

$$3\beta\text{-}Ca_3(PO_4)_2 + Ca(OH)_2 \rightarrow Ca_{10}(PO_4)_6(OH)_2 \quad (R4)$$

The resulting HA was ball-milled for 24 h in a polyurethane-lined ball mill using zirconia milling media, to achieve a median grain size of approximately 0.6 μm

**Table 1** Parameters of the various reference patterns used for the XRD analysis, taken from database PDF-2®

| | HA | | $\beta$-TCP | |
|---|---|---|---|---|
| Pattern No. | 09-0432 | 74-0566 | 09-0169 | 70-2065 |
| Crystal system | Hexagonal | Hexagonal | Rhombohedral | Rhombohedral |
| Space group | $P6_3/m$ | $P6_3/m$ | R-3C | R3C |
| a (Å) (=b) | 9.418 | 9.424 | 10.429 | 10.439 |
| c (Å) | 6.884 | 6.879 | 37.38 | 37.375 |
| RIR | None | 1.06 | None | 1.25 |

(see Table 1), and XRD and FTIR were used to confirm its phase purity.

Although under-reported, this HA synthesis technique is relatively simple and inexpensive compared to standard precipitation methods [30].

### 2.2 BCP sample preparation

HA and $\beta$-TCP (Fluka No. 21218) powders were combined to form batches with $\beta$-TCP contents of 0, 20, 40, 50, 60, 80 and 100 wt% (balance HA), hereafter referred to as BCP-*n*, where *n* indicates the $\beta$-TCP content in weight percent. These batches were mixed in deionised water slurries using a high speed Silverson homogeniser, and then dried for 15 h at 100 °C. A 10 wt% binder phase of PEG 400 diluted in ethanol (1 part PEG 400 to 4 parts ethanol) was hand mixed into the powder, and dried overnight at 60 °C, with several interim repeat stirrings to maintain a homogenous binder distribution during ethanol evaporation.

The powder agglomerates were then sieved below 250 µm, and green bodies uniaxially pressed at 10 MPa in a 40 mm diameter die at room temperature. These were then sintered (pressureless) in air for 1 h at the following soak temperatures: 850, 1000, 1150 and 1300 °C. The temperature cycle up and down rates were fixed at 100 °C per hour.

In addition to this broad composition and sintering temperature survey, several duplicate samples ($n = 5$) were prepared from BCP-60 sintered at 1000 °C for repeat runs, and another series of furnace runs was carried out on BCP-50 and BCP-80 with narrower temperature increments around what appeared to be a critical temperature. Some additional furnace runs were also carried out in a 5% $H_2$ in $N_2$ atmosphere saturated with water vapour.

### 2.3 Sample characterisation

All samples were analysed using XRD (Philips, Cu-K$\alpha$, 45 kV, 40 mA), FTIR (Thermo Nicolet, 400–4000 $cm^{-1}$ range, 4 $cm^{-1}$ resolution) and TGA/SDTA (Mettler Toledo 851E), both before and after sintering.

For the XRD measurements, a $2\theta$ scan range of either 4–70° (phase identification) or 25–38° (phase content quantification), with 0.02° steps and 10 s counts per step was used. The X'Pert HighScore® analysis package was used to quantify the HA/$\beta$-TCP phase content ratio by the method of Chung et al. [31] using the Powder Diffraction File® database (PDF) reference patterns 74-0566 (HA) and 70-2065 ($\beta$-TCP). These patterns were used because they have the relative intensity ratios (RIR) necessary for the quantitative analysis, whereas the more commonly used 09-0432 (HA) and 09-0169 ($\beta$-TCP) patterns do not. The important parameters of each, taken from database PDF-2® Set 53, are listed in Table 1 for comparison.

To support this analysis, the HA/$\beta$-TCP phase content ratios were also quantified using the method of Raynaud et al. [32], who established an XRD-based peak area calibration curve for samples of known HA and $\beta$-TCP contents. That is, the Raynaud et al. method was specifically designed to quantify the phase content ratios of BCP material, whereas the Chung et al. method can be applied to any crystallographic phase.

## 3 Results

### 3.1 HA synthesis by solid state reaction

XRD analysis of the pure HA (i.e. BCP-0) synthesised by solid state reaction revealed single phase crystalline HA, with all peaks identified by PDF® pattern 74-0566. As shown in Fig. 1, this pattern fits the relative intensities of the three dominant HA peaks found at $2\theta = 31.8°$ (211), 32.2° (112) and 32.9° (300) better than the more commonly used pattern 09-0432 which predicts equal peak intensity for the (112) and (300) peaks.

FTIR spectroscopy revealed the standard HA infrared absorption spectrum with the $OH^-$ stretching mode peak at 3571 $cm^{-1}$, and the characteristic peaks and bands between 500-1150 $cm^{-1}$ assigned to $PO_4^{3-}$ (see, for example, [26, 29, 33, 34]). The absorbance spectrum is presented in Fig. 2.

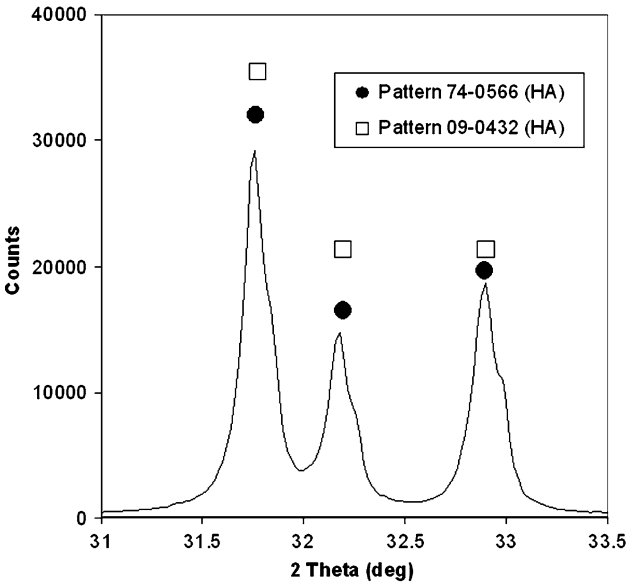


**Fig. 1** Dominant XRD peaks of the HA produced by solid state reaction

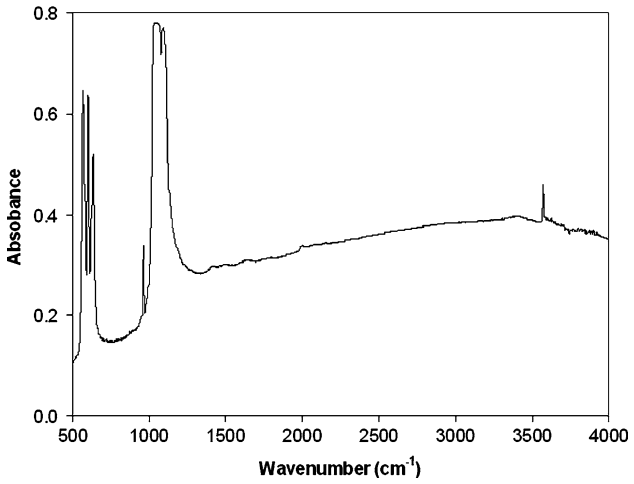


**Fig. 2** FTIR absorbance spectrum of the solid state reaction-produced HA

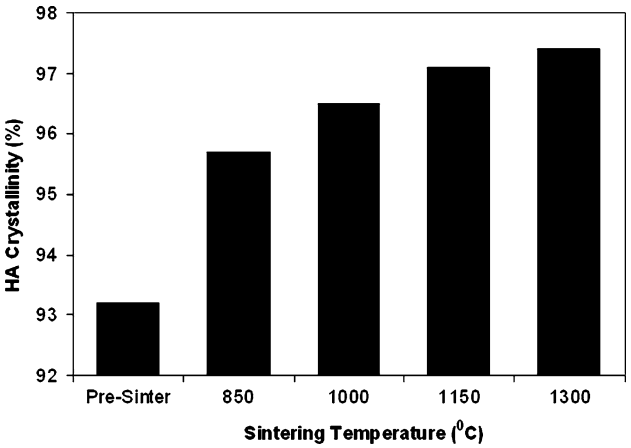


**Fig. 3** Crystallinity of the solid state reaction-produced HA after sintering

The Ca/P molar ratio of the HA was measured by energy dispersive spectroscopy (EDS) with an INCA Analyzer (coupled to a Leo 1525 scanning electron microscope) to be 1.71 ± 0.09. Notwithstanding the fact that EDS is not the most accurate technique for measuring elemental concentrations, the stochiometric value of 1.67 for pure HA lies within this range.

The particle size distributions of the HA and Fluka $\beta$-TCP powders were measured by laser light scattering (Saturn DigiSizer 5200 for the HA and Omec LS-CWM for the $\beta$-TCP), and the main distribution parameters are given in Table 2.

The degree of crystallinity ($X_c$) of the HA pre- and post-sintering was determined by applying Eq. 1 [35] to the relevant XRD diffractograms:

$$X_c \approx 1 - \left(\frac{V_{112/300}}{I_{300}}\right) \quad (1)$$

where $V_{112/300}$ is the height of the valley between the (112) and (300) peaks and $I_{300}$ the intensity of the (300) peak. As shown in Fig. 3, $X_c$ ranged from approximately 93% for the as-synthesised HA (i.e. pre-sintering, but post-reaction R4), to approximately 97% post-sintering at 1300 °C.

**Table 2** Particle size distribution parameters (μm) of the starting powders used for BCP production

| (μm) | D10 | D50 | D90 |
|---|---|---|---|
| HA | 0.25 | 0.59 | 1.31 |
| $\beta$-TCP | 1.66 | 5.72 | 12.57 |

## 3.2 BCP phase content quantification pre-sintering

The HA/$\beta$-TCP phase content ratios of the BCP samples were measured using two complementary XRD-based methods: the Chung et al. method [31] (via the X'Pert HighScore® analysis package) and the Raynaud et al. method [32], hereafter referred to as C-analysis and R-analysis respectively.

The validity of this approach to phase content quantification was tested by using it to measure and verify against the known pre-sinter $\beta$-TCP contents of the samples. As shown in the calibration curves of Fig. 4, both methods gave satisfactory linear fits with gradients ($m$) very close to

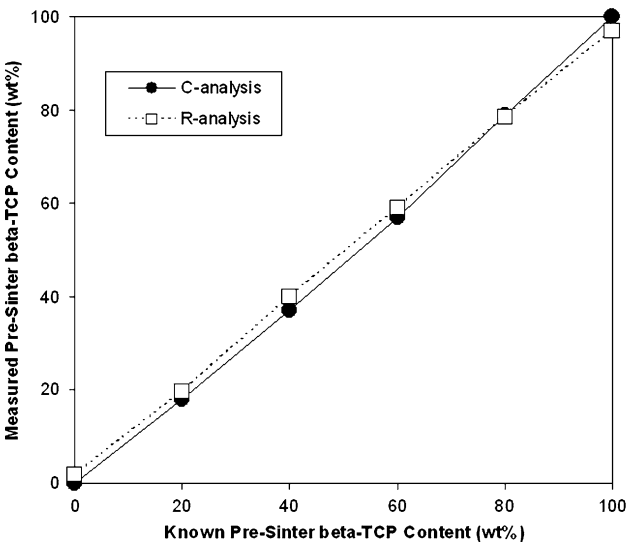


**Fig. 4** Calibration curves of the measured versus known $\beta$-TCP contents for the various BCP samples pre-sintering, using the methods of Chung et al. [31] (C-analysis, solid line) and Raynaud et al. [32] (R-analysis, dashed line)

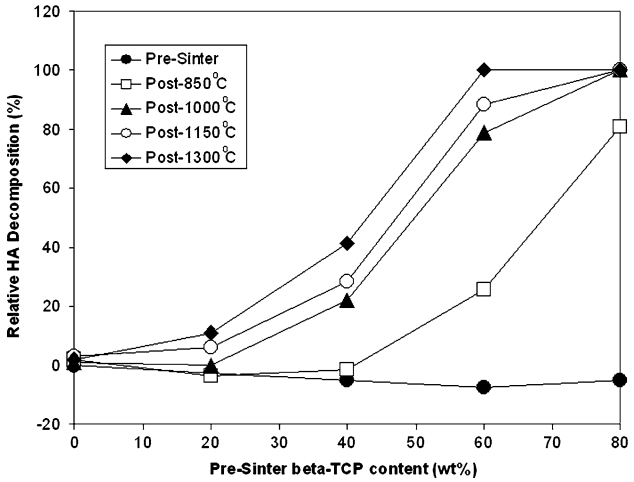


**Fig. 5** Relative HA decomposition quantified by XRD for the BCP samples sintered at different temperatures for 1 h. An error of approximately 5% is expected

unity (C-analysis: $m = 1.004$, R-analysis: $m = 0.959$, $R^2 = 0.999$ for both).

### 3.3 BCP phase content quantification post-sintering

XRD measurements of the BCP samples post-sintering revealed a general decrease in HA intensity relative to the known pre-sinter HA contents, always with an associated increase in $\beta$-TCP intensity. No crystalline phases other than HA and $\beta$-TCP were identified in the sintered samples, so the results suggest the thermal decomposition of some of the HA to $\beta$-TCP during sintering. Results of the C-analysis are presented in Fig. 5 as the measured relative HA decomposition (i.e. (pre-sinter HA – post-sinter HA)/pre-sinter HA × 100%) against the known pre-sinter $\beta$-TCP content. (The R-analysis gave almost identical results to the C-analysis, so it is not included in Fig. 5 for clarity.)

As no thermal decomposition is expected before sintering, the pre-sinter data in Fig. 5 (solid circles) give an indication of the typical error expected using this approach to quantifying the relative extent of decomposition (approximately 5%), and reflects the slight deviation from unity gradient recorded in Fig. 4. Nevertheless, the data convincingly show the extent of thermal decomposition to be greater at higher sintering temperatures, but even more so for higher pre-sinter $\beta$-TCP contents. For example, only 3% decomposition is recorded for BCP-0 (0 wt% $\beta$-TCP) after sintering at 1150 °C and above, whereas 80% decomposition is recorded for BCP-80 (80 wt% $\beta$-TCP) at the relatively low sintering temperature of 850 °C. Although the value of 3% is below the approximately 5% error expected from this approach, the presence of $\beta$-TCP in the BCP-0 sample post-sintering was unambiguously identified, as shown in Fig. 9. It therefore appears that the presence of $\beta$-TCP strongly promotes the thermal decomposition of HA to $\beta$-TCP.

In the case of BCP-60, approximately 80% of the initial HA content decomposed to $\beta$-TCP during sintering at 1000 °C (i.e. from a pre-sinter HA content of 40 wt% to a post-sinter content of 8 wt%). This is unexpectedly high given that 1000 °C is a relatively mild sintering temperature for bioceramics. Several independent repeat BCP-60 samples ($n = 5$) were produced and analysed as before to verify this, and, as shown in Fig. 6, the collected XRD diffractograms indeed confirmed the observation. Both C-analysis and R-analysis yielded approximately 80% decomposition (Fig. 7), in good agreement with the data in Fig. 5.

To determine whether the HA decomposition could be the result of the solid state reaction method of HA synthesis, and, in particular, to the high levels of residual stress expected in the HA grains after the ball-milling stage, repeat measurements were also carried out on BCP-60 samples produced using (i) the HA annealed at 1000 °C for 18 h post-milling, and (ii) commercially available HA (Merck No. 1.02196). Both yielded similar results to that shown in Fig. 7 post-sintering at 1000 °C, confirming that the decomposition is not related to the HA synthesis route. Similarly, a high temperature annealing of the $\beta$-TCP powder (1000 °C for 18 h) prior to BCP synthesis was found to have no effect on the HA decomposition.

Repeat tests were also carried out on BCP-50 and BCP-80 with narrower soak temperature increments than the broad survey of Fig. 5. The results are presented in Fig. 8.

Again the C-analysis and R-analysis results agree well for both samples. For BCP-80, the decomposition starts sharply around 800 °C with a rapid conversion with increased sintering soak temperature to the final value,

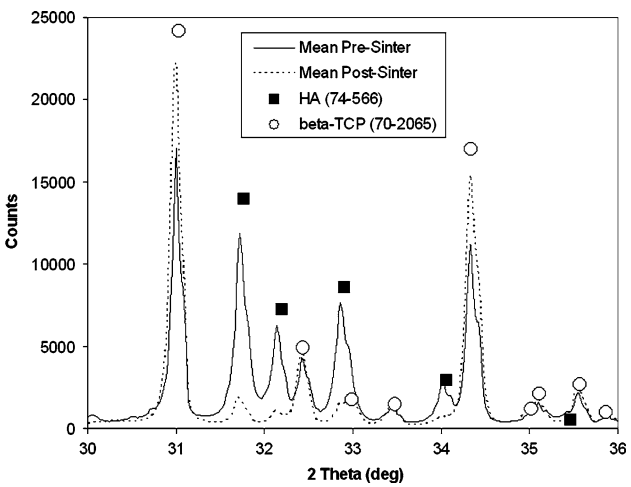


**Fig. 6** Mean XRD diffractograms for the repeat ($n = 5$) BCP-60 samples pre- (solid line) and post-sintering (dashed line) at 1000 °C

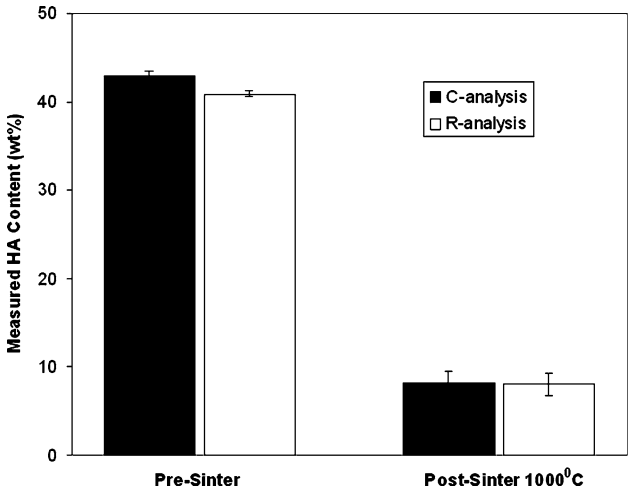


**Fig. 7** C- and R-analysis results for the repeat BCP-60 samples. Error bars indicate ± standard deviation ($n$ = 5)

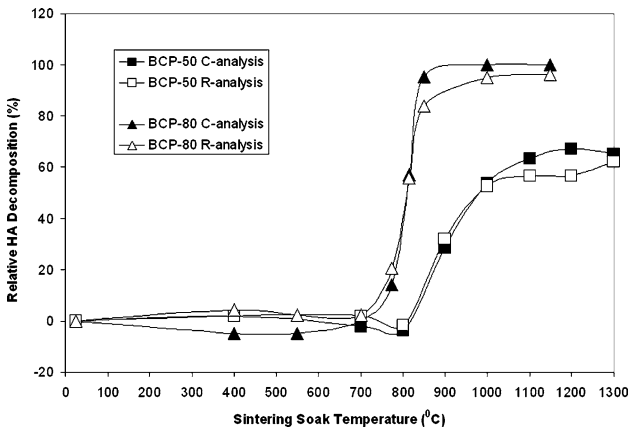


**Fig. 8** XRD determination of the critical temperature for the thermal decomposition of HA to $\beta$-TCP in BCP-50 and BCP-80

whereas for BCP-50, the onset is again clear, but the conversion is more gradual with sintering soak temperature, occurring over the range between approximately 800 °C and 1100 °C.

While no α-TCP was detected in any of the samples sintered below 1300 °C, it was indeed identified in the XRD diffractograms (pattern 09-0348) of some of the samples sintered at 1300 °C. Pattern 09-0348 does not have the RIR necessary for phase content quantification by C-analysis, but plotting the intensities of the dominant peaks of HA, $\beta$-TCP and α-TCP at 31.77°, 31.02° and 30.71° ($2\theta$) respectively is nevertheless informative (Fig. 9). The peak intensities in Fig. 9 have been normalised to the HA peak intensity of BCP-0.

α-TCP was detected in BCP-20, BCP-40 and BCP-60 sintered at 1300 °C, with the α-TCP content increasing with increasing starting $\beta$-TCP content up to BCP-60. At pre-sinter $\beta$-TCP contents greater than 60 wt%, however, no α-TCP was detected.

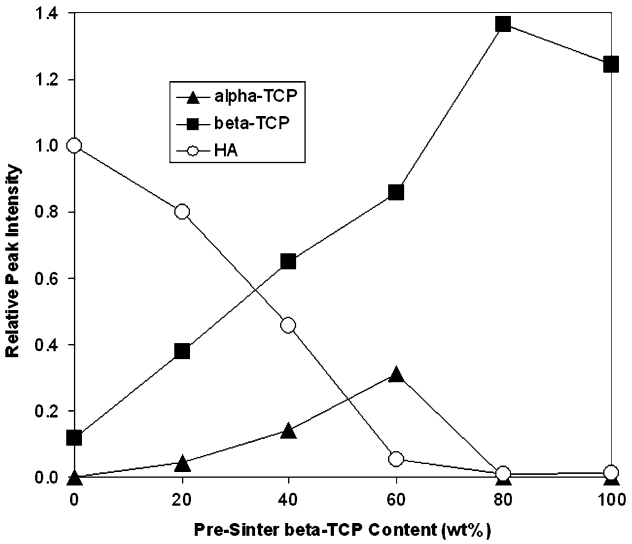


**Fig. 9** Relative dominant peak intensities of the HA, $\beta$-TCP and α-TCP phases (see text for peak positions) for the BCP samples sintered at 1300 °C

The sintered BCP samples were also characterised with FTIR, wherein the absorbance peak at 3571 $cm^{-1}$ assigned to the stretching mode of the hydroxyl group in the HA lattice was found to diminish in intensity with higher sintering temperature, disappearing completely after sintering at 1300 °C. This HA lattice dehydroxylation was also observed for BCP-0, with almost complete dehydroxylation achieved after sintering at 1300 °C (Fig. 10). Recall, however, that the extent of decomposition to $\beta$-TCP for this sample as measured by XRD (Fig. 5) after the same thermal treatment was only approximately 3%.

TGA/SDTA measurements were carried out in flowing air on three samples: BCP-0, BCP-50 and BCP-100. The approximately 10 wt% binder in the powder is seen to burn

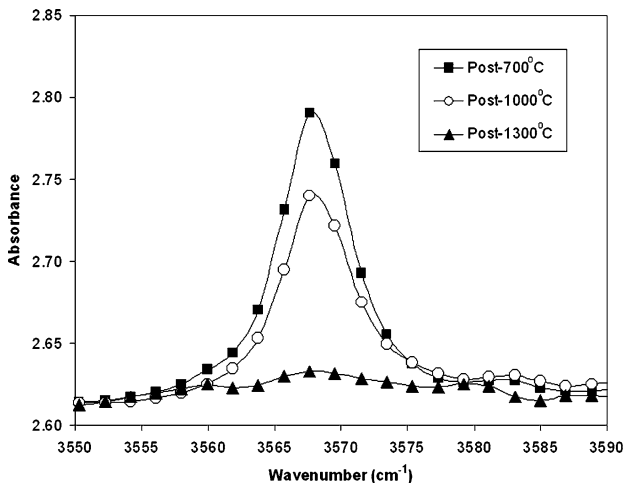


**Fig. 10** The $OH^-$ peak of the FTIR spectrum for BCP-0 (pure HA) after sintering at various temperatures

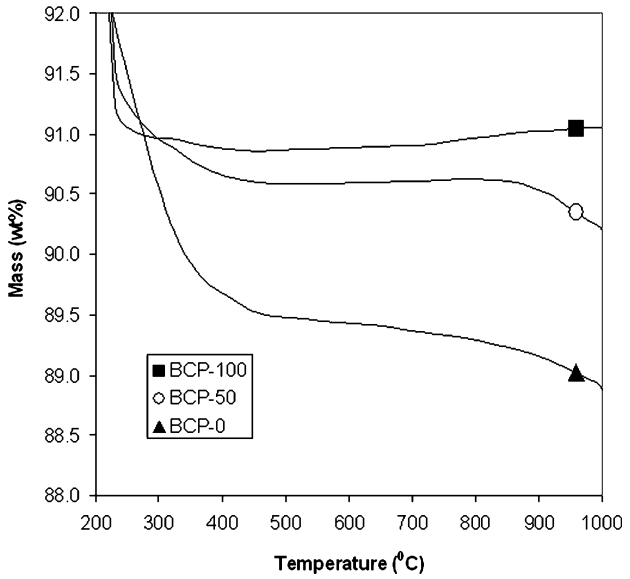


**Fig. 11** TGA measurements of BCP-0, 50 and 100

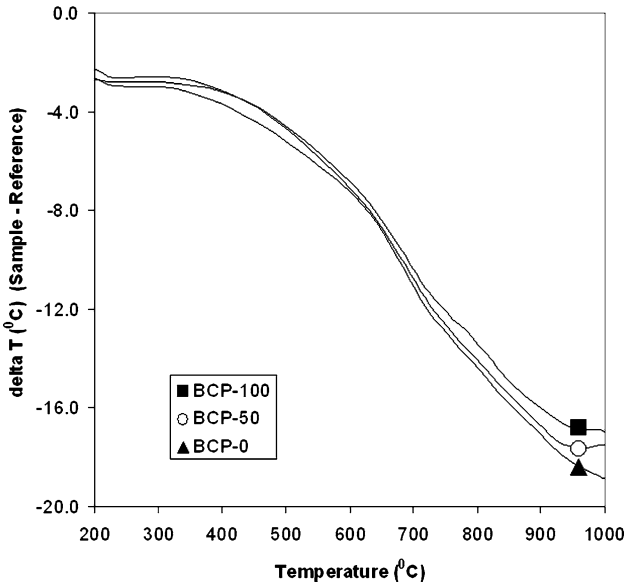


**Fig. 12** SDTA measurements for BCP-0, 50 and 100, where delta *T* is the sample temperature minus the reference temperature

off by 400 °C in the TGA traces of Fig. 11. A steady mass loss is then observed for the BCP-0, whereas BCP-50 displays a more abrupt onset of mass loss above 800 °C.

The corresponding SDTA curves for the data in Fig. 11 gave no indication of any particular reactions occurring around what is believed to be the critical temperature range of 800–1100 °C, as noted in Fig. 8. The curves did however indicate that the systems are endothermic with ΔT in the –16 °C to –19 °C range at 1000 °C (Fig. 12). Importantly, no distinctive peak around 790 °C was observed in any of the SDTA measurements, despite trying several different heating rates ranging from 0.1 °C.min$^{-1}$ to 2.5 °C.min$^{-1}$. This peak is associated with the transformation of Ca-deficient apatite to $\beta$-TCP [17, 19], as described by reaction R2, so the BCP-0 data in Fig. 12 (solid triangles) suggests that the solid state reaction-produced HA is not Ca-deficient.

As reaction R1 was considered to be the most likely channel for the observed HA decomposition (albeit via the formation of OHAP and OHA interim phases), a careful XRD search for the presence of either CaO or $Ca(OH)_2$ in the BCP-60 sample post-sintering at 1000 °C was considered. However, the only significant XRD peak for either species that is not obscured by more dominant HA or $\beta$-TCP peaks is the 71% intensity $Ca(OH)_2$ peak at 18.07° ($2\theta$), and in a separate calibration exercise, the detectability limit for $Ca(OH)_2$ at this peak position was found to lie between 5 wt% and 10 wt% (balance $\beta$-TCP). Recalling that approximately 80% of the pre-sinter HA content of BCP-60 (i.e. 40 wt%) decomposed to $\beta$-TCP (Fig. 7), if the process was fully described by reaction R1, a $Ca(OH)_2$ content of 2.4 wt% would result. Because this is below the detection limit, XRD confirmation of reaction R1 was not possible in the present study.

Some additional furnace runs in a sintering atmosphere of 5% $H_2$ in $N_2$ bubbled through water (hereafter referred to as 'humid atmosphere') were carried out on BCP-60 to investigate the effect of sintering atmosphere on the HA decomposition. For direct comparison with the air-sintered results of Fig. 7, the same temperature profile was used, i.e. a 1 h soak at 1000 °C with a 100 °C per hour ramp rate.

Starting with a pre-sinter HA content of 40 wt% (i.e. BCP-60), an HA content of 27 wt% was measured post-sintering in the humid atmosphere. Recall that only 8 wt% HA was recorded post-sintering in air (Fig. 7), so the humid atmosphere significantly reduced the rate of HA thermal decomposition. Interestingly, by sintering in humid atmosphere the BCP-60 sample that had already undergone air sintering, increased its HA content from 8 wt% to 15 wt%, indicating a partial recovery of the thermally decomposed HA.

## 4 Discussion

HA synthesis by solid state reaction is demonstrated to be effective and relatively simple, with single phase purity confirmed by XRD and FTIR, and a degree of crystallinity greater than 97% achieved after sintering at 1150 °C. As suggested by Fazan et al. [30], this HA synthesis route offers an attractive alternative to the more commonly used precipitation methods.

The complementary methods of Chung et al. [31] and Raynaud et al. [32] for the XRD-based quantification of the

HA/β-TCP phase content ratio of BCP material are found to agree well. Using this approach, the thermal decomposition of HA to β-TCP was observed and quantified in BCP samples with a wide compositional range after sintering at several different temperatures. For example, approximately 80% of the pre-sinter HA content of BCP-60 (40 wt%) decomposed to β-TCP after sintering at 1000 °C. This is particularly striking given that 1000 °C is a relatively mild sintering temperature for bioceramics.

The fact that only approximately 3% of the pure HA sample decomposed at 1300 °C (as confirmed by XRD), but underwent almost complete dehydroxylation at this temperature (as confirmed by FTIR), suggests that with increasing temperature, dehydroxylation is the first process to begin in the HA lattice, subsequently followed by decomposition to β-TCP. This agrees with the findings of Meejoo et al. (2006) [36] who observed the onset of dehydroxylation of nano-HA particles at 700 °C, then the formation of β-TCP above 800 °C. It is also consistent with the now generally accepted view that the thermal decomposition of HA to β-TCP occurs via the interim formation of OHAP, then OHA [24, 25], phases that still retain the lattice structure of HA, and are therefore indistinguishable from HA with XRD.

It is well established that the starting material stochiometry also plays a critical role in determining the thermal stability of the various calcium phosphate phases [26–28, 37, 38]. For example, Raynaud et al. [26] reported reaction R2 for Ca-deficient apatite after sintering at 700 °C. Although no clear evidence of non-stochiometry in the HA powder prepared by solid state reaction was found by either EDS or TGA/SDTA, the possibility of slight non-stochiometry cannot be ruled out because neither technique is conclusive. In the case of a slight non-stochiometry, reaction R2 could contribute, at least in part, to the observed HA decomposition. However, the fact that the same thermal decomposition effect was also observed for BCP material prepared with commercially available HA (instead of the in-house prepared HA) further suggests that the HA stochiometry cannot be considered a dominant contributing factor.

In good agreement with the findings of Wang et al. [39], sintering in an atmosphere saturated with water vapour reduced the extent of HA decomposition significantly, and reversed it under certain conditions (although not completely). As summarised by Heimann [24], this is consistent with the rehydroxylation of OHA to HA, and further supports the view that the thermal decomposition of HA to β-TCP observed in this study occurs via the dehydroxylation of HA to the interim OHAP, then OHA phases.

The HA decomposition rate was found to be strongly promoted by increased levels of initial (i.e. pre-sintering) β-TCP. Indeed, the decomposition of pure HA (BCP-0) to β-TCP during sintering at 1300 °C for 1 h was found to be only approximately 3%, whereas almost 100% decomposition was recorded for the HA present in BCP-60 after the same treatment. This supports the contention of Kivrak et al. [16] that a β-TCP content beyond a certain critical level "acts as a driving force for the further decomposition of the HA phase through dehydroxylation." The initial β-TCP levels in the BCP mixes were also found to influence the temperature range over which the extent of thermal decomposition reached a maximum. The critical role the initial β-TCP content appears to play in these observations is somewhat surprising and currently not understood. One hypothesis is that intimate contact between the HA and β–TCP grains achieved during sintering leads to high stresses at the grain boundaries, partly arising from the thermal expansion coefficient mismatch between HA and β-TCP, particularly along the c-axis (as observed by Nakumura et al. [40]). This thermal expansion coefficient mismatch stress is believed to promote the thermal decomposition of the HA phase.

The agreement between the temperatures of transformation, as were observed in the present study, with the temperature range where the dehydroxylation of HA occurs as is reported in the literature, is noticeable. This therefore suggest that the presence of β-TCP influences the dehydroxylation of HA, which sets in motion a series of decomposition steps that eventually leads to β-TCP as an end product. What the exact mechanism is, is not clear at this stage. Further studies need to be undertaken to illucidate this matter.

The detection of α-TCP in some of the samples sintered at 1300 °C is not surprising considering the confirmed β-TCP → α-TCP transformation above 1125 °C (R3), but does indicate that the reverse transformation (α-TCP → β-TCP) expected upon gradual cooling did not go to completion in these samples. Somewhat surprising, however, is that for the BCP material with pre-sinter β-TCP content greater than 60 wt%, no α-TCP is observed after sintering at 1300 °C, suggesting complete α-TCP → β-TCP reverse transformation in these samples. This may indicate that for BCP material, if the HA content is below a certain critical level, the α-TCP → β-TCP reverse transformation goes to completion, and above this level it is retarded. If this is the case, the results suggest that this critical HA content lies somewhere between 20 wt% and 40 wt%.

## 5 Conclusion

HA powder was synthesised by solid state reaction between β-TCP and $Ca(OH)_2$ at 1000 °C. XRD and FTIR confirmed the single phase purity of the HA, and its crystallinity was calculated to be 93% post-synthesis, increasing to 97%

post-sintering at 1150 °C for 1 h. A suite of BCP materials comprising an intimate mix of this HA and $\beta$-TCP with a wide range of HA/$\beta$-TCP phase content ratios was then produced by mechanical intermixing, then sintering at several different temperatures. The aim of the study was to investigate the thermal stability of the BCP material during sintering by XRD, FTIR and TGA/SDTA.

Combining the XRD-based methods of Chung et al. [31] and Raynaud et al. [32], thermal decomposition of HA to $\beta$-TCP in the sintered BCP was identified and quantified, and the decomposition process was found to be strongly promoted by higher $\beta$-TCP contents in the starting mixes. For example, as much as 80% of the pre-sinter HA content of BCP-60 (40 wt%) decomposed to $\beta$-TCP by sintering at 1000 °C for 1 h, with the onset of decomposition occurring around 800 °C. It is postulated that the catalytic effect the $\beta$-TCP has on the HA thermal decomposition is due to the thermal expansion coefficient mismatch between the intimately mixed phases. The decomposition process could be retarded, and under certain conditions, reversed, by sintering in a water vapour saturated atmosphere. FTIR measurements indicated that dehydroxylation of the HA lattice accompanies its ultimate decomposition to $\beta$-TCP. All the results are consistent with the now generally accepted view that the thermal decomposition of HA proceeds via the interim formation of firstly OHAP, then OHA. The presence of $\beta$-TCP therefore could influence the dehydroxylation rate of the HA and thus the cascade of decomposition reactions of the HA, leading to the observed phenomena. Furthermore, the pre-sinter HA content appeared to influence the reverse transformation of $\alpha$-TCP to $\beta$-TCP expected upon gradual cooling from temperatures greater than 1125 °C.

Because the HA/$\beta$-TCP phase content ratio dominantly determines the rate and extent of BCP resorption in vivo, and considering the clear risk of this ratio changing during synthesis, its determination post-synthesis is critical. This is particularly relevant if the synthesis involves high temperature treatment.

**Acknowledgements** One of the authors (RN) would like to thank the SRP of the Council for Scientific and Industrial Research (CSIR) for funding this study on the YREF program. The XRD and FTIR measurements were carried out at the National Metrology Laboratory of the CSIR, with assistance from Retha Rossouw and Eino Vuorinen respectively.

## References

1. G. DACULSI, R. Z. LEGEROS, E. NERY, K. LYNCH and B. KEREBEL, *J. Biomed. Mater. Res.* **23** (1989) 883
2. U. RIPAMONTI, *Biomaterials* **17** (1996) 31
3. M. VALLET-REGI and J. M. GONZALEZ-CALBET, *Progr. Solid State Chem.* **32** (2004) 1
4. S. YAMADA, D. HEYMANN, J. M. BOULER and G. DACULSI, *Biomaterials* **18** (1997) 1037
5. G. DACULSI, *Biomaterials* **19** (1998) 1473
6. T. LIVINGSTONE ARINZEH, T. TRAN, J. MCALARY and G. DACULSI, *Biomaterials* **26** (2005) 3631
7. P. HABIBOVIC, H. YUAN, C. M. Van Der VALK, G. MEIJER, C. A. Van BLITTERSWIJK and K. De GROOT, *Biomaterials* **26** (2005) 3565
8. J. M. CURRAN, J. A. GALLAGHER and J. A. HUNT, *Biomaterials* **26** (2005) 5313
9. R. AYERS, S. NIELSEN-PREISS, V. FERGUSON, G. GOTOLLI, J. J. MOORE and H. J. KLEEBE, *Mater. Sci. Eng. C* **26** (2005) 1333
10. D. LE NIHOUANNEN, G. DACULSI, A. SAFFRAZADEH, O. GAUTHIER, S. DELPLACE, P. PILET and P. LAYROLLE, *Bone* **36** (2005) 1086
11. C. E. WILSON, M. C. KRUYT, J. D. De BRUIJN, C. A. Van BLITTERSWIJK, F. CUMHUR ONER, A. J. VERBOUT and W. J. A. DHERT, *Biomaterials* **27** (2006) 302
12. E. GOYENVALLE, E. AGUADO, J. M. NGUYEN, N. PASSUIT, L. LE GUENENNEC, P. LAYROLLE and G. DACULSI, *Biomaterials* **27** (2006) 1119
13. W. SUCHANEK and M. YOSHIMURA, *J. Mater. Res.* **13** (1998) 94
14. Z. YANG, Y. JIANG, Y. WANG, L. MA and F. LI, *Mater. Lett.* **58** (2004) 3586
15. A. CÜNEYT TAS, F. KORKUSUZ, M. TIMUCIN and N. AKKAS, *J. Mater. Sci. Mater. Med.* **8** (1997) 91
16. N. KIVRAK and A. CÜNEYT TAS, *J. Am. Ceram. Soc.* **81** (1998) 2245
17. I. R. GIBSON, I. REHMAN, S. M. BEST and W. BONFIELD, *J. Mater. Sci. Mater. Med.* **11** (2000) 533
18. E. CAROLINE-VICTORIA and F. D. GNANAM, *Trends Biomater. Artifi. Organs* **16** (2002) 12
19. S. H. KWOM, Y. K. JUN, S. H. HONG and H. E. KIM, *J. Euro. Ceram. Soc.* **23** (2003) 1039
20. S. KANNAN, J. H. G. ROCHA, J. M. G. VENTURA, A. F. LEMOS and J. M. F FERREIRA, *Scripta Mater.* **53** (2002) 1259
21. J. ZHOU, X. ZHANG, J. CHEN, S. ZENG and K. De GROOT, *J. Mater. Sci. Mater. Med.* **4** (1993) 83
22. H. LI, B. S. NG, K. A. KHOR, P. CHEANG and T. W. CLYNE, *Acta Mater.* **52** (2004) 445
23. S. DYSHLOVENKO, C. PIERLOT, L. PAWLOWSKI, R. TOMASZEK and P. CHAGNON, *Surface Coat. Technol.* **201** (2006) 2054
24. R. B. HEIMANN, *Surf. Coat. Technol.* **201** (2006) 2012
25. C. J. LIAO, F. H. LIN, K. S. CHEN and J. S. SUN, *Biomaterials* **20** (1999) 1807
26. S. RAYNAUD, E. CHAMPION, D. BERNACHE-ASSOLLANT and P. THOMAS, *Biomaterials* **23** (2002) 1065
27. C. P. A. T. KLEIN, J. G. C. WOLKE and K. DE GROOT, in "An Introduction to Bioceramics", edited by L. L. HENCH and J. WILSON (World Scientific Publishing, 1993) p. 199
28. R. Z. LEGEROS and J. P. LEGEROS, in "An Introduction to Bioceramics", edited by L. L. HENCH and J. WILSON, (World Scientific Publishing, 1993) p. 139
29. R. RAMACHANDRA RAO, R. RAI, H. N. ROOPA and T. S. KANNAN, *J. Mater. Sci. Mater. Med.* **8** (1997) 511
30. F. FAZAN and K. B. N. SHAHIDA, *Med. J. Malaysia* **59** (2004) 69
31. F. H. CHUNG, *Journal of Applied Crystallography* **7** (1974) 513
32. S. RAYNAUD, E. CHAMPION, D. BERNACHE-ASSOLLANT and J.-P. LAVAL, *J. Am. Ceram. Soc.* **84** (2001) 359
33. F.-H. LIN, L. CHUN-JEN, C. KO-SHAO and S. JUI-SHENG, *Mater. Sci. Eng. C* **13** (2000) 97

34. A. RAPACZ-KMITA, C. PALUSZKIEWICZ, A. SLOSARCZYK, Z. PASKIEWICS, *J. Mol. Struct.* **744–747** (2005) 653
35. E. LANDI, A. AMPIERI, G. CELOTTI and S. SPRIO, *J. Eur. Ceram. Soc.* **20** (2000) 2377
36. S. MEEJOO, W. MANEEPRAKORN and P. WINOTAI, *Thermochim. Acta* **447** (2006) 115
37. G. MURALITHRAN and S. RAMESH, *Ceram. Int.* **26** (2000) 221
38. M. DESCAMPS, J. C. HORNEZ and A. LERICHE, *J. Eur. Ceram. Soc.* (2006). In press (doi:10.1016/j.jeurceramsoc.2006.09.005)
39. P. E. WANG and T. K. CHAKI, *J. Mater. Sci. Mater. Med.* **4** (1993) 150
40. S. NAKUMURA, R. OTSUKA and H. AOKI, *Thermochim. Acta* **165** (1990) 57